Green Chemistry Letters and Reviews

ISSN: (Print) (Online) Journal homepage: https://www.tandfonline.com/loi/tgcl20

Enhancing the anticorrosion performance of mild steel in sulfuric acid using synthetic non-ionic surfactants: practical and theoretical studies

Metwally Abdallah, Nizar El Guesmi, Arej S. Al-Gorair, Refat El-Sayed, Aseel Meshabi & Mohamed Sobhi

To cite this article: Metwally Abdallah, Nizar El Guesmi, Arej S. Al-Gorair, Refat El-Sayed, Aseel Meshabi & Mohamed Sobhi (2021) Enhancing the anticorrosion performance of mild steel in sulfuric acid using synthetic non-ionic surfactants: practical and theoretical studies, Green Chemistry Letters and Reviews, 14:2, 382-394, DOI: 10.1080/17518253.2021.1921858

To link to this article: https://doi.org/10.1080/17518253.2021.1921858

Published online: 25 May 2021.

GREEN CHEMISTRY LETTERS AND REVIEWS
2021, VOL. 14, NO. 2, 382–394
https://doi.org/10.1080/17518253.2021.1921858

Taylor & Francis
Taylor & Francis Group

REVIEW

OPEN ACCESS Check for updates

Enhancing the anticorrosion performance of mild steel in sulfuric acid using synthetic non-ionic surfactants: practical and theoretical studies

Metwally Abdallah [a,b], Nizar El Guesmi[a,c], Arej S. Al-Gorair[d], Refat El-Sayed[a,b], Aseel Meshabi[a] and Mohamed Sobhi[b,e]

[a]Chemistry Department, Faculty of Applied Sciences, Umm Al-Qura University, Makkah, Saudi Arabia; [b]Chemistry Department, Faculty of Science, Benha University, Benha, Egypt; [c]Chemistry Department, Faculty of Science, University of Monastir, Monastir, Tunisia; [d]Chemistry Department, College of Science, Princess Nourah Bint Abdulrahman University Libraries, Riyadh, Saudi Arabia; [e]Chemistry Department, Faculty of Science, University of Tabuk, Tabuk, Saudi Arabia

ABSTRACT

The anticorrosion potency of Sabic mild steel (MS) in 0.5 M H_2SO_4 solution was enhanced by three synthetic non-ionic surfactants (NI Surf.) containing pyridine and pyrimidine derivatives. These compounds are safe, environmentally friendly, and harmless to human health. Chemical and electrochemical measurements were used to compute the corrosion parameters. The anticorrosion efficacy increases with increasing the concentration of NI Surf. and with lowering temperature, surface and interfacial tension, and critical micelle concentration. The effectiveness of anticorrosion is interpreted due to the spontaneous horizontal adsorption on the surface of MS by the existence of some active centers that facilitate the adsorption. The adsorption process obeys Temkin isotherm. Potentiodynamic polarization elucidated that the synthetic NI Surf. acted as mixed-type inhibitors. Some surface properties were determined and confirm the anticorrosive effect of these molecules. Quantum chemical parameters as reactivity descriptors were carried out. It should be noted that the results obtained from computational calculations of the specifications are in full agreement with the experimental observations. There is good compatibility between the anticorrosion efficiency obtained from various techniques and surface properties and quantum chemical calculation.

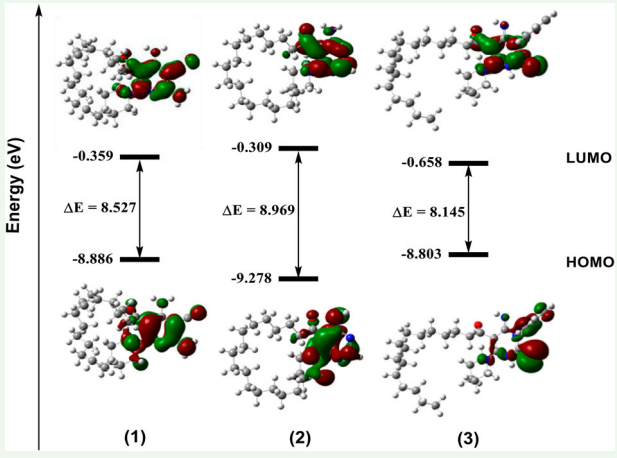

ARTICLE HISTORY
Received 30 November 2020
Accepted 19 April 2021

KEYWORDS
Mild steel; polarization; adsorption; DFT; quantum calculation; surface properties

1 . Introduction

Sabic Mild steel (MS) is utilized in multiple industrial applications, but when exposed to sulfuric acid, it corrodes, causing countless economic losses. Therefore, scientists are trying to find ways to solve the risk of corrosion. The main one is the use of corrosion inhibitors. In previous research, a lot of organic compounds have been used that contain a lot of active groups and oxygen, nitrogen, and sulfur atoms, which facilitate the adsorption process and consequently the corrosion rate reduces, Unfortunately, these compounds have bad effects on human health and the environment (*1*–

CONTACT Metwally Abdallah maabdelsaid@uqu.edu.sa; metwally555@yahoo.com Chemistry Department, Faculty of Applied Sciences, Umm Al-Qura University, Makkah, Saudi Arabia

14). There are several factors that influence the effectiveness of inhibition of organic compounds, such as the type of metal, the chemical composition of the additives, the active groups in the molecule, the temperature, and many other factors (15, 16 17).

Most of the organic compounds give high inhibition efficacy, but unfortunately these compounds are high in price and harmful to human health and the environment. And to create inhibitors that are safe, environmentally friendly for humans, and give high efficiency in preventing steel from corrosion attack. One of these inhibitors that solve these problems is the use of nonionic surfactants that are inexpensive, easy to dissolve in water, and have a high adsorption capacity on the steel surface (18–22). Some non-ionic surfactant molecules were utilized to protect some metals from the corrosion process in acidic solutions as the previous work by Abdallah et.al. (23–28).

The strategic objective of this manuscript is to try to inhibit the corrosion of MS in 0.5 M H_2SO_4 solution using nonionic surfactants (NI Surf.) containing pyridine and pyrimidine derivatives. The selected concentration (0.5 M HCl) is the suitable concentration for the pickling and chemical cleaning of MS. Weight reduction (WR), electrochemical impedance spectroscopy (EIS), and potentiodynamic polarization (PP) measurements were used in this study. Also, the impact of rising temperature on the dissolution of MS in devoid of and containing NI Surf. molecules were investigated. The relationship between the anticorrosion efficiency and the surface parameters with quantum chemical calculations is also explicated.

2 . Experimental

2.1. Chemical and electrochemical measurements

MS was applied in this study to conduct chemical and electrochemical experiments and its chemical composition as follows (weight %) carbon = 0.072, manganese = 0.610, phosphor = 0. 041, silicon = 0.041, vanadium = 0.020, and the rest iron.

For weight reduction experiments (WR) A mild steel coupon with dimensions of $2 \times 3 \times 0.1$ cm was used and for potentiodynamic polarization (PDP) and electrochemical impedance (EIS), MS sample rod immersed in Araldite with the denuded surface area of 0.38 cm^2, Before any experience the MS coupons or rod surface furbished with a diverse degree of emery papers (ranged from 200 to 1200). Finally, it is dried with a fine filter paper. The method of WR measurements is done as mentioned previously (29).

For PDP and EIS techniques, three-compartment cell containing MS as working electrode, Pt foil used as auxiliary electrode, and saturated calomel electrode (SCE) as reference electrode A PS remote Potentiostat with PS6 software was used to determine the corrosion parameters obtained from the PDP measurements. *EIS* measurements were accomplished at a frequency range from 10 kHz to 100 mHz and signal amplitude perturbation of 5 mV by using a computer-controlled potentiostate (Auto Lab 30, Metrohm). All the measurements were performed at a temperature of 30 ± 1°C by using ultra circulating thermostat.

2.2. Synthesis of pyridine and pyrimidine derivatives (I–III) as nonionic surface-active agents

This design was carried out by the following process:

Process 1. *Synthesis of pyridine 1 and pyrimidine derivatives 2, 3*

Reaction of enaminonitrile derivative [prepared by stirring of malononitrile (0.01 mol) in dry ethanol for 2 h with palmitoyl chloride (0.01 mol) to give the malononitrile intermediate, followed by heating for 3 h with piperidine to yield the enaminonitrile derivative] in boiling DMF (20 mL) with the presence of base catalyst and malononitrile, phenyl isothiocyanate and/or formamide produced the pyridine 1 and/or pyrimidine derivatives 2,3, respectively (Scheme 1).

Process 2. *Preparation of nonionic surfactants (I–III) from pyridine and pyrimidine (1–3)*

Addition of propylene oxide (10 moles) to the products (1–3) by fusion in presence of KOH, in each case gave surf (I–III), respectively (Scheme 2). The amount of propylene oxide, which reacted was determined by the gain in weight of the mixture after the addition.

The composition of all the products was established based on the spectra of IR with ^{1}HNMR.

Pyridine derivative (1): IR: 3337–3194 ($2NH_2$), 2915, 2848 (14 CH_2), 2216 (C≡N), 1700 (C=O). ^{1}H NMR: 0.87 (t, 3H, CH_3), 1.24–1.59 (m, 28H, $14CH_2$), 1.62 (m, 6H, $3CH_2$), 3.39 (m, 4H, $2CH_2$), 6.72 (s, 2H, NH_2), 7.82 (s, 2H, NH_2).

Pyrimidine derivative (2): IR: 3407, 3201 (NH_2), 2915, 2848 ($14CH_2$), 1698 (C=O). ^{1}H NMR: 0.87 (t, 3H, CH_3),

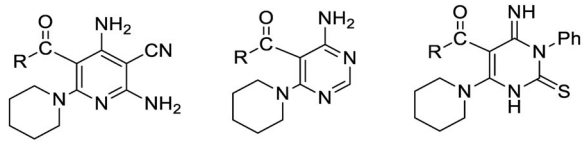

R = $CH_3(CH_2)_{14}$

Scheme 1 The pyridine **1** and/or pyrimidine derivatives **2,3**.

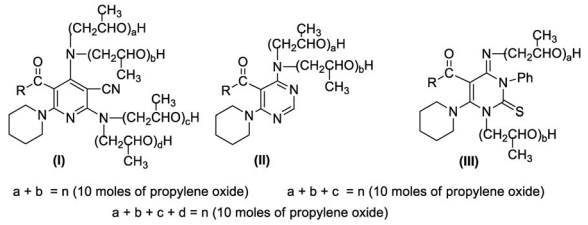

Scheme 2. Nonionic surfactants **(I–III)** from pyridine and pyrimidine **(1–3)**.

1.31–1.34 (m, 28H, $14CH_2$), 1.61 (m, 6H, $3CH_2$), 2.34 (m, 4H, $2CH_2$), 7.82 (s, 2H, NH_2), 8.83 (s, 1H, CH=N).

Pyrimidine derivative (3): IR: 3306, 3195 (2NH), 2915, 2849 (14 CH_2), 1684 (C=O). ^{1}H NMR: 0.83 (t, 3H, CH_3), 1.34–1.55 (m, 28H, $14CH_2$), 1.63 (m, 6H, $3CH_2$), 2.34 (m, 4H, $2CH_2$), 7.25–7.70 (m, 6H, ArH and NH), 10.99 (s, 1H, NH).

NI Surf. I: IR: The (OH) group of propoxy chain absorbed at 3405 as a broad band, and (C–O–C) ether of poly propoxy (EPP)chain at 1104, 914; ^{1}H NMR: The propoxy protons ($CH_2CH(CH_3)O$) appeared in region (3.01–3.90) as a multiple signals, beside the other signals of the target.

NI Surf. II: IR: The (OH) group of propoxy chain absorbed at 3389 as a broad band, and (C–O–C) EPP chain at 1107, 919.

NI Surf. III: IR: The (OH) group of propoxy chain absorbed at 3393 as a broad band, and (C–O–C) EPP chain at 1103, 911; ^{1}H NMR: The propoxy protons (CH2CH(CH_3)O) observed in region (3.22–3.80) as a multiple signals, beside the other signals of the target.

2.3. Estimation of surface characteristics

Some of the surface characteristics of the three non-ionic surfactants were assigned as previously defined (*30*, *31*), the surface tension S. T (γ), interfacial tension (IFT) critical micelle concentration (CMC), the efficiency (π_{cmc}), the surface excess (Γ_{max}), the surface area (A_{min}), the free energy of micellization (ΔG°_{mic}) and adsorption (ΔG°_{ads}) properties were measured at 25°C and depicted in Table 1.

2.4. Computational methods

All the calculations have been accomplished with the Gaussian 03 suite of programs. Geometry optimizations were carried out on **1–3** *in vacuo* with hybrid density functional theory (DFT) using Lee–Yang–Parr (B3LYP) exchange–correlation functional theory, together with the standard 6–31G (d) basis set. Frequency calculations were also carried out on the optimized geometries using the same level of theory.

3 . Results and discussion

3.1 WR measurements

3.1.1 . Impact of NI surf. concentration

Figure 1 represents the relationship between the WR and time for MS coupons in free 0.5 M H_2SO_4 solution and contains some concentrations (ranging from 50 to 250 ppm) of NI Surf. III molecule at 298 K. Like curves were acquired for the other two NI Surf. molecules but not shown and the corrosion data are recorded in Table 2. It is evident that with increasing the concentration of these molecules, the WR values decreased. This suggests that NI Surf exists retard the corrosion rate of MS in 0.5 M H_2SO_4 solution or in another meaning, these molecules act as corrosion inhibitors. The linear relationship in Figure 1 due to insoluble surface films during corrosion (*32*).

The rate of corrosion $R_{corr.}$ ($g.cm^{-2}.min^{-1}$) the surface coverage (θ) and the anticorrosion efficiency % *AE* were determined from the subsequent equation and listed in Table 1 (*33*).

$$R_{corr} = \Delta W/St \quad (1)$$

$$\%AE = [1 - R_{add}/R_{free}]100 = \theta \times 100 \quad (2)$$

where ΔW is the weight reduction ($\Delta W = W_a - W_b$), W_a and W_b are the weight of MS before and after exposure to the corrosive solution, *S* is the surface area and *t* is the inundation time, R_{free} and R_{add} are the corrosion rate in free 0.5 M H_2SO_4 solution and including NI Surf., respectively.

% *AE* increases with increasing concentration of NI Surf. by increased the adsorbed surfactant molecules at the MS surface and increase the amount of covering area.

Obviously from Table 2, the R_{corr} value was lowered and the % *AE* values increased, confirming the inhibiting strength of the NI Surf. molecules. % *AE* also increases with increased NI Surf. concentration. This is due to an

Table 1. Surface properties of the synthesized compounds.

Surf.	S T (γ) (dyne/cm) 0.1 wt%	IFT (dyne/cm) 0.1wt%	CMC (mM/L^{-1})	π_{cmc} (dyne/cm)	$\Gamma_{max} \times 10^{-3}$ (mol/m^2)	$A_{min} \times 10^{-5}$ nm^2	$-\Delta G^{o}_{mic}$ (KJ/m)	$-\Delta G^{o}_{ads}$ (KJ/m)
NI Surf. I	39.2	10.6	0.42	31.2	1.40	1.18	13.555	13.552
NI Surf. II	38.1	9.4	0.34	32.0	1.46	1.43	14.228	14.226
NI Surf. III	36.4	8.3	0.28	34.6	1.57	1.05	14.308	14.305

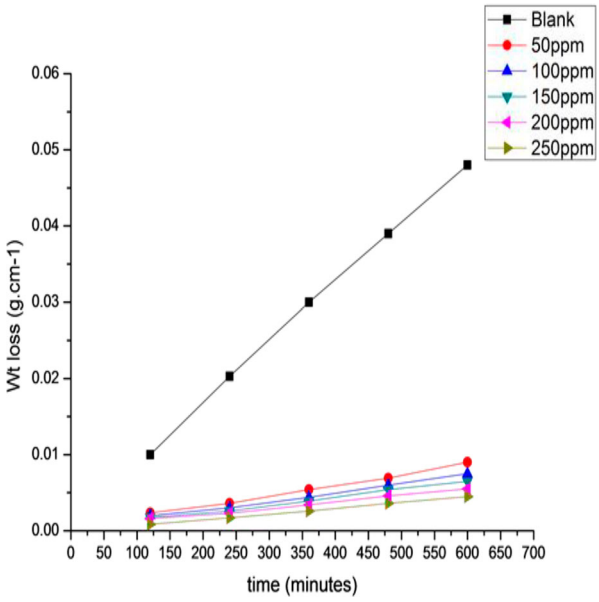

Figure 1. WR-time curves for corrosion of MS in free 0.5 M H_2SO_4 solution and containing some concentration of NI Surf. III.

increased adsorption of NI Surf. on the surface of MS and an increase in the coverage area. The sequence of % *AE* at the same surfactant concentration decreases in the subsequent arrangement:

$$\text{NI Surf.III} > \text{NI Surf.II} > \text{NI Surf.I}$$

3.1.2. Impact of temperature

The impact of rising temperature (from 298 to 328 K) on the R_{corr} and *AE* % of the MS coupons free 0.5 M H_2SO_4 solution and the presence of 250 ppm of NI Surf. molecules have been studied. Similar curves to Figure 1 were obtained but invisible. Corrosion parameters are registered in Table 3. It is apparent from this table, by increasing the temperature from 298 to 328 K, R_{corr} increases and reduced *AE* % values donate a good inhibition efficacy at 298°C. This due to the desorption of NI Surf. molecules from the MS surface at higher temperatures. The increase in R_{corr} values with high temperature signalizes the physical adsorption of NI Surf. molecules on the surface of the MS. The corrosion of MS in 0.5 M H_2SO_4 is an activation-controlled chemical reaction, the $R_{corr.}$ greatly affected by temperature. Typically, R_{corr}, increases significantly as temperature increases. Activation polarization is usually the controlling factor during corrosion of MS in strong acids. Certainly the rate determination step is not a chemical reaction because the corrosion in the present state and as clearly shown by the experimental results is simple absorption. In addition, the cathodic reaction in this study is the H_2 evolution. Therefore, the diffusion-controlled source is excluded.

Table 2. Corrosion data obtained from WR measurements for MS in free 0.5 M H_2SO_4 solution and containing different concentrations of NI Surf. molecules.

NI Surf.	Conc. (ppm)	$R_{cor} \times 10^{-5}$ (mg cm^{-2} min^{-1})	θ	% *AE*
Blank	0	6.76	–	–
NI Surf. I	50	1.12	0.834	83.43
	100	0.96	0.857	85.79
	150	0.83	0.877	87.72
	200	0.75	0.889	88.90
	250	0.66	0.902	90.23
NI Surf. II	50	1.15	0.829	82.98
	100	1.03	0.847	84.76
	150	0.92	0.863	86.39
	200	0.76	0.887	88.75
	250	0.64	0.905	90.53
NI Surf. III	50	1.43	0.788	78.84
	100	1.20	0.822	82.24
	150	1.07	0.841	84.17
	200	0.72	0.893	89.34
	250	0.54	0.920	92.01

Table 3. Influence of the increasing temperature on the R_{corr} and % *AE* obtained from WR protection.

NI Surf.	Temperature (°K)	$R_{cor.} \times 10^{-5}$ (mg cm^{-2} min^{-1})	% *AE*
0.5 M H_2SO_4	298	6.76	–
	308	7.40	–
	318	8.76	–
	328	10.70	–
NI Surf. I	298	0.66	90.23
	308	1.6	78.37
	318	2.54	71.00
	328	3.8	64.48
NI Surf. II	298	0.64	90.53
	308	1.3	82.43
	318	2.5	71.46
	328	3.1	71.02
NI Surf. III	298	0.54	92.01
	308	0.88	88.10
	318	1.9	78.31
	328	2.8	73.83

Activation thermodynamic parameters such as the activation energy (E_a*), the enthalpy of activation ΔH* and the entropy of activation ΔS* for the dissolution of MS in 0.5 M H_2SO_4 solutions of and containing 250 ppm of the examined NI Surf. molecules were computed using Arrhenius equation (*34*, *35*):

$$R_{corr} = A \exp(-E_a^*/RT) \quad (3)$$

$$R_{corr} = RT/Nh \exp(\Delta S^*/R) \exp(-\Delta H^*/RT) \quad (4)$$

where A is constant depends on the electrode and the electrolyte, R is the gas constant T is the temperature, h is the Plank's constant and N is the Avogadro's number.

Figure 2 displays the Arrhenius plot of log R_{corr} versus 1/T of MS in free 0.5 M H_2SO_4 solutions and contains 250 ppm of NI Surf. examined. The values of E_a* can be determined from slope of the straight lines and equal to 18.42 kJ mol^{-1} for the free 0.5 M H_2SO_4 and

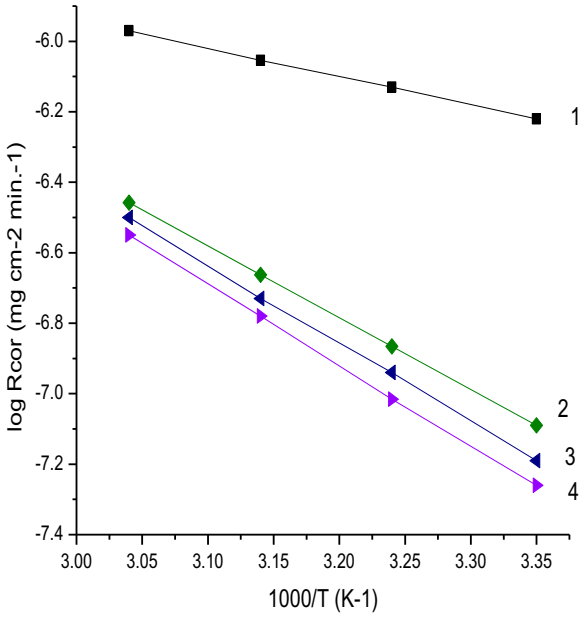

Figure 2. The relationship between log R_{cor} versus 1/T curves for MS in the blank 0.5 M H_2SO_4 solution and when containing 250 ppm of NI Surf. molecules. (1) 0.5 M H_2SO_4 (2) 0.5 M H_2SO_4 + 250 ppm NI Surf. I (3) 0.5 M H_2SO_4 + 250 ppm NI Surf. II (4) 0.5 M H_2SO_4 + 250 ppm NI Surf.III.

equal to 34.39, 36.58, and 37.91 kJ $mol^{-1}$for the NI Surf. I, II, and III, respectively.

The presence of NI Surf. molecules increased the E_a* values due to a significant lowering in the adsorption process of the NI Surf. molecules on the surface of MS with increasing temperature and increase in the reaction rate due to exposure of a large area of MS to H_2SO_4 solution. In addition, tested NI Surf. molecules act as an inhibitor by increasing activation energy of MS corrosion by creating a barrier to mass and charge transfer by adsorption onto the surface of MS.

Figure 3 represents a plot of log (R_{corr} /T) vs1/T of uninhibited MS in 0.5 M H_2SO_4 and inhibited by NI Surf. molecules. A straight line with a slope of (−ΔH*/2.303 R) and an intercept of [log (R/Nh) + ΔS*/2.303 R].

The values of ΔH* obtained from the slope of the straight line equal to and equal to 17.32 kJ mol^{-1} for the free 0.5 M H_2SO_4 and equal to 30.18, 32.24, and 34.62 kJ mol^{-1}in the presence of the NI Surf. molecules I, II, and III, respectively. The positive sign of ΔH* reflects that the adsorption of the NI Surf. molecules on the MS surface are an endothermic process. The values of ΔS*obtained from the intercept of a straight line and to −196.24 J mol^{-1} K^{-1} for the free 0.5 M H_2SO_4 and equal to −197.23, 198.33, and 199.64 J mol^{-1} $K^{-1}$for the surfactants molecules I, II, and III respectively. The signs of ΔS* in the free and presence of NI Surf. molecules are negative. This demonstrates that the activation complex is a rate-determining step that represents binding rather than secession indicates a reduction in perturbation on the transition from the reactants to the activated complex (*36*).

3.2. PP measurement

PP curves for MS in blank 0.5 M H_2SO_4 solutions and contain various concentrations (ranging from 50 to

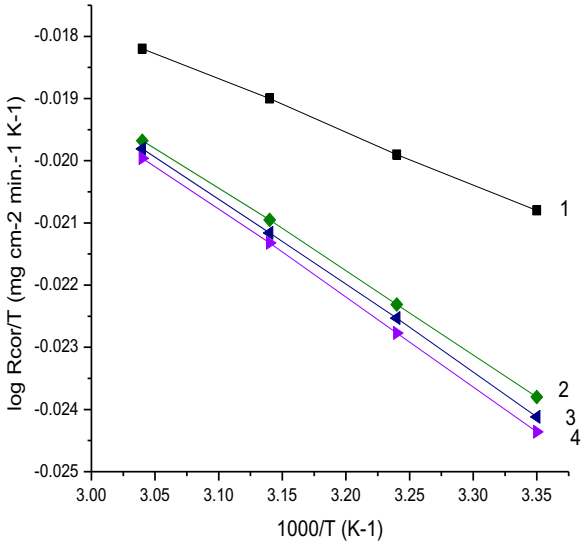

Figure 3. The relationship between log R_{cor}/T versus 1/T curves for MS in the blank 0.5 M H_2SO_4 solution and containing 250 ppm of NI Surf. molecules. (1) 0.5 M H_2SO_4 (2) 0.5 M H_2SO_4 + 250 ppm NI Surf. I (3) 0.5 M H_2SO_4 + 250 ppm NI Surf. II (4) 0.5 M H_2SO_4 + 250 ppm NI Surf. III.

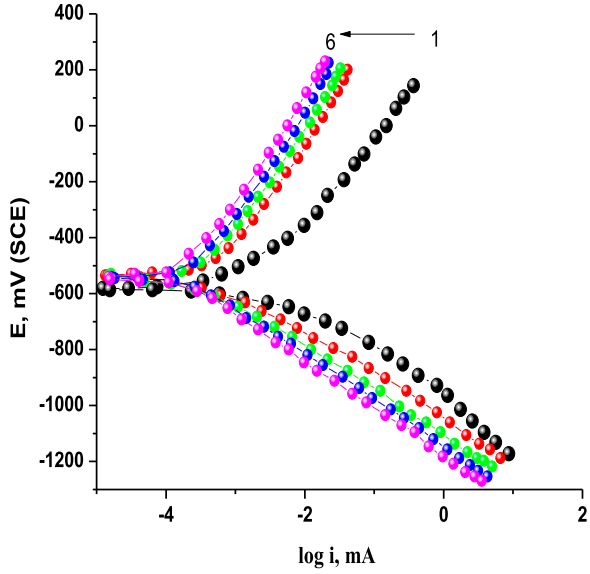

Figure 4. PDP curves for the dissolution of MS electrode in free 0.5 M H_2SO_4 solution and contain different concentrations of NI Surf. III.

Table 4. Corrosion parameters obtained from the PP curves.

NI Surf. concentration	β_a, mV dec^{-1}	β_c mV dec^{-1}	$-E_{corr}$, V (SCE)	$I_{corr.} \times 10^{-4}$ mA cm^{-2}	% *AE*
0.5 M H_2SO_4	346	291	0.54	1.65	–
0.5 M H_2SO_4 + NI Surf.I 50ppm	361	292	0.54	0.255	84.54
100 ppm	359	293	0.52	0.234	85.82
150 ppm	358	296	0.52	0.195	88.20
200 ppm	358	296	0.52	0.179	89.15
250 ppm	353	299	0.53	0.136	91.76
0.5 M H_2SO_4 + NI Surf. II 50 ppm	362	298	0.54	0.262	84.12
100 ppm	358	293	0.54	0.237	85.64
150 ppm	355	297	0.54	0.198	88.00
200 ppm	355	288	0.53	0.163	90.12
250 ppm	354	293	0.52	0.138	91.64
0.5M H_2SO_4 + NI Surf. III 50 ppm	356	288	0.54	0.328	80.12
100 ppm	362	293	0.54	0.277	83.21
150 ppm	362	296	0.52	0.233	85.87
200 ppm	361	294	0.52	0.156	90.54
250 ppm	357	298	0.53	0.109	93.39

250 ppm) of NI Surf. III molecule with a sweep rate of 2 mV/s are represented in Figure 4. Similar curves for NI Surf. I and NI Surf. II molecules were obtained but were not shown and the corrosion data were registered in Table 4. By examining this Figure, it is apparent that the anodic and cathodic polarization curves were shifted to lower values of the current density upon adding any of the tested NI Surf. molecules. This result demonstrates the inhibitory activity of all molecules tested for MS corrosion in 0.5 M H_2SO_4 solutions.

The kinetic corrosion parameters e.g. corrosion potential (E_{corr}), corrosion current density (I_{corr}), anodic and cathodic Tafel slope (β_c) determined from the curves are inserted in Table 4. Some observations, due to the addition of the NI Surf. molecules examined, E_{corr} values are not affected by adding tested NI Surf. molecules. The values of I_{corr} lowered, and the % *AE* increase with increasing of the NI Surf. concentration. As the NI Surf. concentration increases in the bulk solution, The amount of particles adsorbed on the surface of MS increases, which leads to an increase in anticorrosion efficacy. Both β_a and β_c values are almost constant. This confirms that NI Surf. molecules acted as an inhibitor of the mixed type. This type of inhibitor works by adsorption of both anodic and cathodic sites on the MS surface and thus delays anodic and cathodic reactions. This behavior reduces the MS corrosion rate. This inhibitory action is due to the forming of an insoluble layer resulting from adsorption of the NI Surf. molecules on the MS surface. The % *AE* is reduced in the following sequence as NI Surf. **III** < NI Surf. **II** < NI Surf. **I**. This sequence is consistent with that obtained from the WR measurement.

3.3. EIS measurements

EIS measurements were applied to examine the inhibition strength of NI Surf. molecules on MS including surface properties, electrode kinetics, and mechanistic information. The impedance spectra of different Nyquist plots were analyzed by relying on the experimental data to a simple equivalent circuit model as elucidate above (37). The Nyquist plots of MS in 0.5 M H_2SO_4 solution free and contain diverse concentrations of NI Surf. III ranged from 50 to 250 ppm at 298°K ± 1 was represented in Figure 5. Like curves for the other two molecules NI Surf. I and NI Surf. II obtained not displayed.

Nyquist impedance does not show a perfect semicircle and is referred to the frequency dispersion due to roughness and heterogeneity of the steel surface. The impedance diagram shows the same direction (single capacitive loop), however, the diameter of this loop increases as the concentration of NI Surf. molecules increase. As a result, the corrosion rate reduces. The increase in the value of R_{ct} due to the adsorption of NI Surf. on the MS surface (*38, 39*). Corrosion inhibition was increased by increasing the NI Surf. concentration.

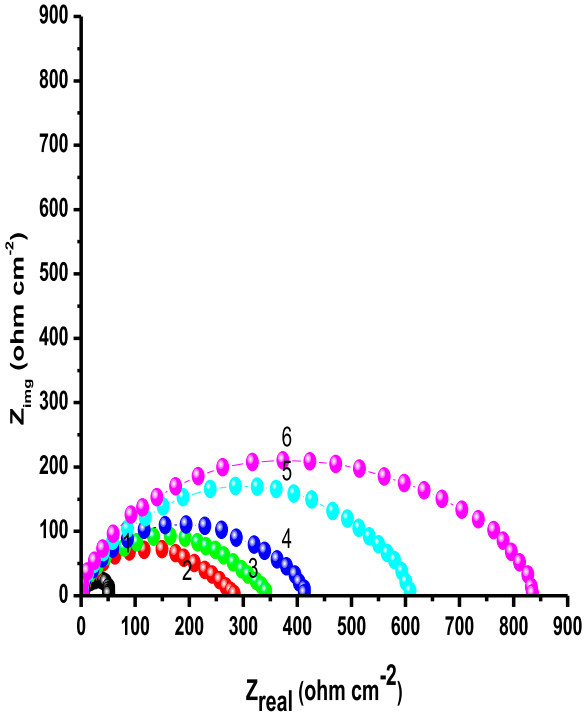

Figure 5. Nyquist diagrams for dissolution of C-steel in 0.5 M H_2SO_4 solutions devoid and containing different concentrations of NI Surf. III.

Table 5. Corrosion parameters obtained by EIS measurements of the MS in free 0.5 M H_2SO_4 solutions and contains some concentrations of NI Surf. molecules.

NI Surf. concentration	R_{ct} (ohm cm^{-2})	$C_{dl} \times 10^{-5}$ (μFcm^{-2})	% *AE*
0.5 M H_2SO_4	56	4.30	– –
0.5 M H_2SO_4 + NI Surf. I 50 ppm	361	0.988	84.51
100 ppm	422	0.783	86.30
150 ppm	491	0.578	88.66
200 ppm	531	0.459	89.45
250 ppm	627	0.383	91.10
0.5 M H_2SO_4 + NI Surf. II 50 ppm	358	1.002	84.35
100 ppm	430	0.789	86.97
150 ppm	477	0.587	88.23
200 ppm	603	0.463	90.71
250 ppm	651	0.381	91.39
0.5 M H_2SO_4 + NI Surf.III 50 ppm	277	0.987	79.78
100 ppm	344	0.766	83.72
150 ppm	412	0.541	86.40
200 ppm	608	0.455	90.78
250 ppm	841	0.378	93.34

The capacity of double layer (C_{dl}) can be computed from the next equation:

$$C_{dl} = 1/2\pi f_{max} R_{ct} \quad (5)$$

where f_{max}. is the maximum frequency.

The percentage anticorrosion efficiencies (% *AE*) of the tested NI Surf. molecules were determined from the following equations:

$$\%AE = [1 - (R_{ct})_f/(R_t)_{in}] \times 100 \quad (6)$$

where $(R_{ct})_f$ and $(R_{ct})_{in}$ are the charge transfer resistance values in the free and existence of NI Surf. molecules. The corrosion parameters obtained from EIS measurements e.g. R_{ct}, C_{dl}, and % *AE* of the investigated NI Surf. are registered in Table 5.

From the data obtained in Table 5. Obviously, with rising the concentration of NI Surf. molecules, R_{ct} values increase owing to the formation of a protective film at the MS/electrolyte interface while Cdl values decrease due to exchange of water molecules at the electrode interface by NI Surf. molecules of lower dielectric constant through adsorption. An increase in % *AE* values suggests that the NI Surf. molecules adsorb on the MS surface and cover several sites of the steel surface forming an adherent layer (*40*).

The anticorrosion efficacy sequence for the tested NI Surf. molecules are reduced as follows: NI Surf. III< NI Surf. II < NI Surf. I. This sequence corresponds to that obtained from the WR and PDP measurement. These results indicate the good compatibility between the different measurements and thus prove the sincerity of the results obtained. The % *AE* values of the investigated NI Surf. molecules are more efficient than other published works such as ethoxylated nonionic surfactants based on Schiff base (*41*). Nonionic surfactants based on propane tricarboxylic acid (*42*) and amino acids based-surfactant molecules, namely, sodium N-dodecyl asparagines (AS), sodium N-dodecylhistidine (HS) and sodium N-dodecyltryptophan (*23*, *24*).

3.4. Adsorption isotherm

Adsorption of the synthesized NI Surf. molecules on the MS surface was accompanied by the removal of water molecules from the surface. The adsorption operation can be thought of as a replacement process in which the NI Surf. molecule in the aqueous phase NI Surf. $_{(aq)}$ replace the 'y' amount of adsorbed water molecules on MS surface according to the following equation (*43*).

$$NI\ Surf._{(aq)} + yH_2O_{(sur)} \rightarrow NI\ Surf_{(s)} + yH_2O_{(aq)} \quad (7)$$

where y is the amount of adsorbed water molecules substituted by a one NI Surf. compound.

Several factors influence the adsorption process, for example, the types of surfactant molecules, the presence of heteroatoms in the chemical composition of surfactant molecules, the type of electrode used, concentration of aggressive acidic solutions, acidity of the solution, temperature, and other factors. The amount of (θ) for some concentrations of three NI Surf. were evaluated from the WR data. The values of θ of different concentrations of the synthesized NI Surf. were utilized to demonstrate the adsorption isotherm of these anticorrosive on the MS surface. Several adsorption isotherms have been applied to interpretation the adsorption behavior of NI Surf. molecules. Temkin isotherm has

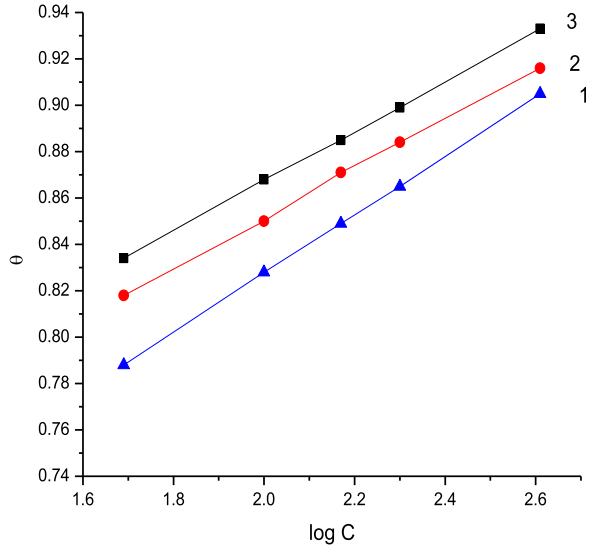

Figure 6. The relation between θ and log C (Temkin isotherm) (1) NI Surf. I (2) NI Surf. II (3) NI Surf. III.

been found to be the better description of adsorption behavior of the NI Surf. molecules on the MS surface, according to the subsequent equation (*17*).

$$\theta = 2303/a(\log K_{ads} + \log C) \quad (8)$$

where K_{ads} is the equilibrium constant of the adsorption, **C** is the NI Surf. concentration, **a** is constant. Figure 6 represents the relationship of θ versus log C which gave a straight line confirming that the adsorption of NI Surf. on the surface of MS in a 0.5 M H_2SO_4 solution at 25°C follows Temkin's adsorption isotherm. The applicability of Temkin's isotherm is achieved by assuming a monolayer adsorption on a homogeneous and uniform metallic surface with an interaction in the adsorption layer. The K_{ads} are computed from the intercept of the straight-line relationship and equal to 24.8, 23.6, and 18.6×10^{-2} for molecules NI Surf. I, NI Surf. II, and NI Surf. III, respectively, demonstrated the more vigor adsorption, and therefore, superior protection for NI Surf. molecules on the surface of MS.

The free energy of adsorption (ΔG°_{ads}) was computed from the subsequent relation (*44*):

$$\Delta G^{\circ}_{ads} = -RT \ln (55.5\, K_{ads}) \quad (9)$$

where the value (55.5) is the molar concentration of water in solution. Generally if the values of $\mathbf{\Delta}G^{\circ}_{ads}$ around −20 kJ/mol or lower. The process can be referred to as the physical adsorption; while those around −40 kJ/molor higher elucidate chemical adsorption. The obtained values of $\mathbf{\Delta}G^{\circ}_{ads}$ are equal to −34.39, −36.58, and −38.36 kJ/mol which demonstrates that the adsorption of NI Surf. on MS surfaces is a mix of physical and chemical adsorption. The high values of ΔG°_{ads} and their negative values indicate that the adsorption reaction of NI Surf. onto the surface of MS is spontaneously and accompanied with a vigor efficient adsorption of such compounds.

3.5. Surface characteristics

An eco-friendly non-ionic surfactant (I–III) was successfully synthesized by an environmentally benign process to the establishment of green chemistry. The surface characteristics such as γ, IFT, CMC, π_{cmc}, Γ_{max}, A_{min}, ΔG°_{mic}, and $\Delta G^{\circ}_{ads,}$ were recorded in Table 1 and showed that the NI Surf**.** III have has higher efficacy than other NI Surf. (I, II) due to reducing the values of γ and IFT. In general, the synthesized products have the capability to diminish the γ, indicating that a great tendency for the output NI Surf. towards the adsorption at the air/water interface. Where the lower IFT values of the tested NI Surf. III indicated the increase of the strength of cohesion between the MS and NI Surf. molecules.

The CMC feature can be identified as the efficacy of NI Surf. molecules, which detects the required amount of NI Surf. to cause maximum reduction of γ. Where, the low value of CMC has excellent emulsification, solubility, and cleaning properties. When the NI Surf. concentration increases, the values of γ decrease steadily and at critical concentrations there is no significant decrease in the γ. This indicates the achievement of saturation in the surface adsorbed layer and the initiation of micelle formation in the bulk. From the outcomes in Table 1, the NI Surf. showed that a sharp decrease of the γ was observed from NI Surf. molecules I to III. The increase in the gained CMC value can be referred to as an increase in the solubility of the NI Surf molecules. The maximum reduction in γ induced by the dissolution of a NI Surf. molecule was determined by the π_{cmc} activity, which became a measure of the activity of the molecule to reduce the γ of water. The results showed that the tested compounds had ability to reduce γ in the aqueous system. The π_{cmc} values of NI Surf. III in Table 1 are higher than NI Surf I and II in parallel with increasing of % *AE* and decreasing of γ and IFT the tested molecules (*26*).

The Γ_{max} activity is very useful in measuring the adsorption efficacy of NI Surf. at the water–air interface. Thus, a material that reduces γ is redundant at or near the surface, that is, when the γ decreases with an increasing surfactant activity, Γ_{max} is positive. Pumping surfactant particles onto boundary surfaces between phases to form an adsorbent layer. The higher values of Γ_{max} and the lower values of A_{min} of NI Surf. III which has more inhibiting efficiency than the other two NI.Surf. molecule demonstrated the vigor aggregation capability at the air–water interface (*30*).

The computed values of (ΔG°_{mic}) and (ΔG°_{ads}) are a negative sign suggest that the two processes are spontaneous. A comparison of the two values showed a slight increase in (ΔG°_{mic}) than (ΔG°_{ads}). The more negative (ΔG°_{ads}) values indicate the NI Surf. emigrate to the interface or aggregate in micelles to minimize the repulsion process and thus the free energy of the system is minimized (*31*).

3.6. Anticorrosion mechanism

The anticorrosive strength of the investigated nonionic surfactants originated from the formation of a protective layer that is adsorbed onto the MS surface. The adsorption process can be attributed to several different factors such as the electron donor hetero atoms, the ring size, and the electron-withdrawn groups in the structure. In

addition, the existence of free lone pairs electron in the N, S atoms and π electron on double bond facilitates the adsorption of the NI Surf. molecules on the MS surface. NI Surf. long chain of hydrocarbons adsorbs it to the MS surface through water-loving (hydrophilic) parts which contain hetero atoms (N, O, and S). Moreover, hydrocarbon chains tend to be warped in water to reduce the contact area between them and the water molecule (*44*).

The anticorrosive mechanism can be elucidated as follows: the long hydrocarbon chain of NI surf. molecules are absorbed on the MS surface by the hydrophilic fractions, which contain oxygen, nitrogen, or sulfur atoms. On the other hand, the hydrocarbon chains tend to wrap in water to reduce the contact area between them and the water molecule. The NI Surf. molecules have a distinct structure composing of a structural group, and they have little attraction to the solvent, known as a hydrophobic group with a group of strong solvent attractiveness (Like water) is called a water-loving group. When the surf. molecules soluble in water, the existence of a hydrophobic group inside the solvent causes the structure of the solvent liquid to be distorted, which increases the system's free energy (*44*). In the aqueous solution, the hydrogen bonding between the water molecules is disfigured by the occurrence of non-polar materials. Thus, water attempted to completely dislodge the nonpolar substances as a separate phase. However, this is not as possible as the hydrophobic group set from NI Surf. hydrated and its expulsion would require blocking the adsorption of the NI Surf. molecules to the surface of MS.

It is apparent that the values of % *AE* acquired from the various techniques demonstrate the sensible anticorrosion efficiency of the NI Surf. for the corrosion of MS in 0.5 M H_2SO_4 solution. This can be discussed according to the bonding strength between the hydrophilic group and the MS is more powerful than that power between expelling a hydrophobic group and the aqueous solution. In these circumstances, a diffusion barrier to chemical and/or electrochemical attack of the solution on MS surface was established and therefore, the % *AE* increases.

Moreover, the high molecular size of these compounds resulted in horizontal adsorption at the surface of MS due to the occurrence of some active center. Furthermore, the presence of electron-withdrawn groups as C=O, C=S, or C≡N resulted in an increase in electron motion leading to a high inhibiting effect on the MS surface.

On the other hand, the structures of NI Surf. molecules have heterogeneous rings like the pyridine ring with the existence of C=O and CN groups in NI Surf. I. and the presence of pyrimidine ring in surf. (II & III). Obviously, the % *AE* computed from all various techniques increases in the following sequence NI Surf. III > NI Surf. II > NI Surf. I This can be explained as follows: Presence of a pyrimidine ring in the chemical composition of NI Surf. (II and III) make them more efficacious than NI Surf. I. The surf. III is more efficacious than surf. II due to the presence of more electron donor atoms such (C=O) and (C=S) in its chemical structure. This leads to an increase in the electron density in the adsorption center which leads to an improvement in the adsorption process and an increase of % *AE*. NI Surf. II is highly efficient than NI Surf. I due to the existence of electron donor atoms and the C=S group in the addition of the presence of pyrimidine ring, which promoted the adsorption process.

3.7. Quantum chemical calculations

The use of Density functional theory (DFT) finds increasing in the last four decades and affords various indices to rationalize and understand chemical structure. The concepts that emerge from this theory have also been widely used to generate a general approach to the description of chemical reactivity (*45–50*). Moreover, quantum chemical methods mark a decisive breakthrough in these efforts and have proven very useful in anti-corrosion studies. In order to predict the reactivity of inhibitor molecules, the quantum chemical properties, such as E_{HOMO}, E_{LUMO}, HOMO–LUMO energy gap (ΔE) were performed and the results are collected in Table 6. It has been shown that the frontier molecular orbital (HOMO and LUMO) has significant importance on the mechanism of adsorption of molecules through electro-donation or electro-acceptation character onto the metallic surface.

It is known that the inhibitor with a higher E_{HOMO} value is joined with more capability of the inhibitor molecule to electron sharing. It has been found that in our case the largest E_{HOMO} corresponds to pyrimidine derivative (**3**) (−8.803) in line with the aforementioned experiments. Thus, we can consider that the pyrimidine derivative (**3**) would reveal a more suitable affinity to the adsorption onto the MS surface through the lone pair electrons located on N and S atom to the vacant iron d-orbital. On the other hand, some authors (*38, 51–55*) have reported a relationship between hardness (η) parameter and stability of the complex formed in which a weak value of the hardness corresponds to more stability of the surface-anticorrosive complex formed. In the same context, smaller values of E_{LUMO} signifies a better ability of the anticorrosive to accept electrons. As can be seen in Table 6, the corresponding

Table 6. Calculated theoretical chemical parameters for anticorrosive (**1–3**).

Descriptors	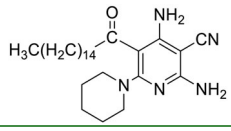	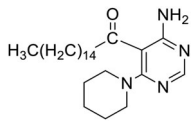	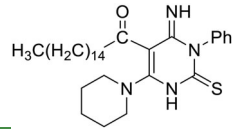
HOMO	−8.886 (eV)	−9.278 (eV)	−8.803 (eV)
LUMO	−0.359 (eV)	−0.309 (eV)	−0.658 (eV)
ΔE(HOMO-LUMO)	8.527 (eV)	8.969 (eV)	8.145 (eV)
Ionization energy (I)	8.886 (eV)	9.278 (eV)	8.803 (eV)
Electron affinity (A)	0.359 (eV)	0.309 (eV)	0.658 (eV)
Dipole moment (Debye)	2.561	1.440	5.224
$\eta = E_L - E_H$	8.527 (eV)	8.969 (eV)	8.145 (eV)
$\mu = (E_H + E_L)/2$	−4.622 (eV)	−4.793 (eV)	−4.731 (eV)
Global softness (σ)	0.117	0.111	0.123
Electronegativity (χ)	4.622 (eV)	4.793 (eV)	4.731 (eV)
$\omega = (-\mu^2/2\eta)$	1.253 (eV)	1.281 (eV)	1.374 (eV)
Electroappcepting (ω^+) power	0.7275	0.7257	0.8915
Electrodonating (ω^-) power	5.350	5.519	5.622
Net electrophilicity ($\Delta\omega^{\pm}$)	6.077	6.245	6.514
ΔN	0.542	0.534	0.581
Fraction of transferred electrons (ΔN)	0.1394	0.1230	0.1393
ΔE back-donation	−2.131	−2.242	−2.036

results for the E_{LUMO} and hardness values follow the same trend in which the pyrimidine derivative (**3**) presents the smaller values of E_{LUMO} and hardness among the anticorrosive studied in this work and consequently indicates a better inhibition efficiency. Furthermore, the greater value of the chemical (σ) softness is also envisageable value, generate the adsorptive tendency of the pyrimidine derivative (**3**) anticorrosive for the MS surface.

On the other hand, in accordance with the frontier molecular orbital theory of chemical reactivity, the separation (ΔE) energy with $\Delta E = E_{LUMO} - E_{HOMO}$, represent a significant parameter as a function of reactivity behavioral inhibition of the anticorrosive molecule towards their adsorption on the MS surface. It is apparent that, as ΔE values decrease, this generates an increase in the reactivity of the anticorrosive molecule and consequently leads to an increase in their inhibition efficiency. The calculated (ΔE) values listed in Table 6 indicate that the pyrimidine derivative (**3**) display the weaker value of $\Delta E = 8.145$, meaning that the inhibitor (**3**) molecule represent the highest reactivity, compared to the other anticorrosive $\Delta E = 8.527$ for (**1**) and $\Delta E = 8.969$ for (**2**) and, consequently, the better inhibition efficiency in accordance with the experimental observations (Figure 7).

It has been revealed also that, the dipole moment parameter depicts another informative quantity that informs us on molecule polarizability with the metal surface. Moreover, it is usually recognized that the anticorrosive efficiency is supposed to be highest for anticorrosive molecules with a greater dipole moment quantity. As expected, and once again in good agreement with the experimentally determined corrosion inhibition efficiency, the dipole moment for pyrimidine derivative (**3**) is 5.224 Debye, proves much greater than for (1) and (2), in which the values are 2.561 and 1.440 Debye, respectively.

The electroaccepting and electrodonating powers, ω^+ and ω^- are defined as (*56*, *57*)

$$\omega^+ = (I + 3A)^2/16(I - A)$$

$$\omega^- = (A + 3I)^2/16(I - A)$$

in which ω^+ and ω^- represents respectively, the measure of the propensity of a given system to accept and to donate charge. It should be noted that a greater value of ω^+ reflects a better capacity of system to accepting charges, while a weaker value of ω^+ corresponds to a favorable electron donor character. Both quantities are determined by employing the vertical ionization energy I and electron affinity A and registered in Table 6.

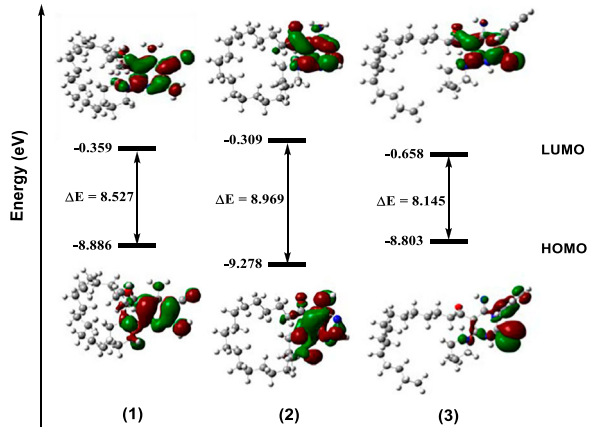

Figure 7 . Optimized structure, HOMO, LUMO surfaces for anticorrosive molecules (**1–3**).

Note that according to these definitions and as mentioned in Table 6 the pyrimidine derivative (**3**) is the molecule with the more capability to donate charge with ω^{-} = 5.622.

The fraction of electrons transferred (ΔN) from the anticorrosive molecule to the metallic atom, can be also calculated by using the equation below (*58–61*)

$$\Delta N = \chi_{Fe} - \chi_{\text{inh}}/2(\eta_{Fe} + \eta_{\text{inh}})$$

where χ_{Fe} and χ_{inh}, η_{Fe} and η_{inh} denotes the absolute electronegativity and hardness of iron and anticorrosive molecule, respectively. The theoretical reported value of $\chi_{\text{Fe}} = 7$ eV and $\eta_{\text{Fe}} = 0$ (*38, 54–56*), owing to the features of the neutral metallic atoms. It is well known that the difference in electronegativity drives the electron transfer. Indeed, electrons displace from the anticorrosive molecules presenting the lower electronegativity value toward metal surface with a greater value of electronegativity, until the chemical potential equilibrium is achieved.

The theoretical values of the fractions transferred are presented in Table 6. It has been found that a great value of ΔN is associated with a high anticorrosive efficiency. Even more, our results indicate a similar previous behavior, since the greater value obtained of Δ*N* corresponds to pyrimidine derivative (**3**) with $\Delta N = 0.581$, showing thus the more effective anticorrosive behavior.

In the literature (*57*), it has been reported that an electronic back-donation process may control the anticorrosive molecule-metallic surface interaction. According to this concept, in the case where the two processes namely charge transfer to the molecule and back-donation from the molecule occurs simultaneously, the change of energy show a direct proportionality to the hardness of the molecule, as defined in the following formula (*62*):

$$\Delta E_{\text{Back}-\text{donation}} = -\eta/4$$

If $\eta > 0$ and $\Delta E_{\text{Back-donation}} < 0$, this implies that back-donation from the molecule to metal is energetically favored. The results reported in Table 6 denote that $\Delta E_{\text{Back-donation}} < 0$ for our anticorrosive molecules (**1–3**), thus the charge transfer to an anticorrosive molecule followed by back-donation from the anticorrosive molecule is energetically favorable. This allows us to make a comparison within inhibiting molecules in relation to their stabilization, knowing that the inhibition efficiency increase in association with better adsorption of the molecule on the metallic surface, and consequently the anticorrosive efficiency ought to increase when the stabilization energy increases resulting from anticorrosive molecule-metallic surface interaction. In consistency with the experimental results and as expected, the calculated $\Delta E_{\text{Back-donation}}$ values display the tendency: (**3**) > (**1**), (**2**).

4. Conclusions

(1) The synthesized NI Surf. molecules were found efficient anticorrosive for MS in 0.5 M H_2SO_4 solutions.
(2) The anticorrosive efficacy increases with the concentrations of the NI Surf. and with decreasing temperature.
(3) The anticorrosive strength of NI Surf. molecules have been attributed to their spontaneous adsorption onto the surface of MS.
(4) The adsorption process is subject to Temkin isotherm.
(5) All surface parameters calculated for NI Surf. molecules and the results of the theoretical calculation are in full agreement with the anticorrosive efficiency of the three molecules examined.

Acknowledgement

The authors would like to thank the Saudi Basic Chemical Industries (SABIC) and the Deanship of Scientific Research at Umm Al-Qura University for supporting this work by Grant Code: (20UQU0030DSR).

Disclosure statement

No potential conflict of interest was reported by the author(s).

ORCID

Metwally Abdallah http://orcid.org/0000-0002-6132-8849

References

[1] Abdel Hameed, R.S.; Al-Bagawi, A.H.; Shehata, H.A.; Shamroukh, A.H.; Abdallah, M. Corrosion Inhibition and Adsorption Properties of Some Heterocyclic Derivatives on C-Steel Surface in HCl. *J. Bio- and Tribo-Corrosion* **2020,** *v51*, 1–11.
[2] El Defrawy, A.; Abdallah, M.; Al-Fahemi, J. Electrochemical and Theoretical Investigation for Some Pyrazolone Derivatives as Inhibitors for the Corrosion of C-Steel in 0.5 M Hydrochloric Acid. *J. Mol. Liq* **2019,** *288*, 110994.
[3] Alfakeer, M.; Abdallah, M.; Fawzy, A. Corrosion Inhibition Effect of Expired Ampicillin and Flucloxacillin Drugs for Mild Steel in Aqueous Acidic Medium. *Int. J. Electrochem. Sci.* **2020**, *15*, 3283–3297.
[4] Suhasaria, A.; Murmu, M.; Satpati, S.; Banerjee, P.; Sukul, D. Bis-benzothiazoles as Efficient Corrosion Inhibitors for Mild Steel in Aqueous HCl: Molecular Structure-Reactivity Correlation Study. *J. Mol. Liq* **2020,** *313*, 113537.

[5] Ferkous, H.; Djellali, S.; Sahraoui, R.; Benguerba, Y.; Behloul, H.; Çukurovali, A. Corrosion Inhibition of Mild Steel by 2-(2-Methoxybenzylidene) Hydrazine-1-Carbothioamide in Hydrochloric Acid Solution: Experimental Measurements and Quantum Chemical Calculations. *J. Mol.Liq.* **2020**, *307*, 112957.
[6] Abdallah, M.; Fawzy, A.; Al Bahir, A. The Effect of Expired Acyclovir and Omeprazole Drugs on the Inhibition of Sabic Iron Corrosion in HCl Solution. *Int. J. Electrochem. Sci.* **2020**, *15*, 4739–4753.
[7] Benghalia, M.A.; Fares, C.; Khadraoui, A.; Meliani, M.H.; Suleiman, R.K.; Sorour, A.A.; Dmytrakh, I.M.; Azari, Z. Assessment of Corrosion Inhibitory Effect of Ruta Chalepensis Flavonoid Extracts on API 5L X52 Steel in 1M HCl Medium. *Env. Eng. and Manag. J* **2019,** *18*, 2009–2021.
[8] Faiz, M.; Zahari, A.; Awang, K.; Hussin, H. Corrosion Inhibition on Mild Steel in 1 M HCl Solution by *Cryptocarya Nigra* Extracts and Three of its Constituents (Alkaloids). *RSC Adv.* **2020**, *10*, 6547–6562.
[9] Abdallah, M.; El-Etre, A.Y.A.; Soliman, M.G.; Mabrouk, E.M. Some Organic and Inorganic Compounds as Inhibitors for Carbon Steel Corrosion in 3.5 Percent NaCl Solution. *Anti-Corros. Meth. Mater* **2006,** *53*, 118–123.
[10] Abdallah, M.; Al–Tass, H.M.; Al-Jahdaly, B.A.; Fouda, A.S. Inhibition Properties and Adsorption Behavior of 5-Arylazothiazole Derivatives on 1018 Carbon Steel in 0.5M H_2SO_4 Solution. *J. Mol.Liq.* **2016**, *216*, 590–597.
[11] Zarrouk, A.; Hammouti, B.; Lakhlifi, T.; Traisnel, M.; Vezin, H.; Bentiss, F. New 1*H*-Pyrrole-2,5-Dione Derivatives as Efficient Organic Inhibitors of Carbon Steel Corrosion in Hydrochloric Acid Medium: Electrochemical, XPS and DFT Studies. *Corros. Sci.* **2015**, *90*, 572–584.
[12] Khadraoui, A.; Khelifa, A.; Hachama, K.; Boutoumi, H. Belkheir Hammouti Synergistic Effect of Potassium Iodide in Controlling the Corrosion of Steel in Acid Medium by Mentha Pulegium Extract. *Res. Chem. Interm* **2015,** *41*, 7973–7980.
[13] Benghaliaa, M.A.; Faresa, C.; Khadraouib, A.; Hadj Meliani a,d, M.; Obotc, I.B.; Sorrourc, A.; Dmytrakhe, M.; Azarid, Z. Performance Evaluation of A Natural and Synthetic Compound as Corrosion Inhibitors of API 5l X52 Steel in Hydrochloric Acid Media. *Mor. J.Chem.* **2018**, *6*, 51–61.
[14] Kamel Hachama, Abdelkader Khadraoui, Mohamed Zouikri, Mohamed Khodja, Abdellah Khelifa, Khadidja Echiker & Belkheir Hammouti Synthesis, Characterization and Study of Methyl 3-(2-oxo-2H-1,4-Benzoxazin-3-yl) Propanoate as New Corrosion Inhibitor for Carbon Steel in 1M H2SO4 Solution, *Res. Chem. Interm.*, **2016**, 42, 987-996.
[15] Morales-Gil, P.; Walczak, M.S.; Ruiz Camargo, C.; Cottis, R.A.; Romero, J.M.; Lindsay, R. Corrosion Inhibition of Carbon-Steel with 2-Mercaptobenzimidazole in Hydrochloric Acid. *Corros. Sci.* **2015**, *101*, 47–55.
[16] Abdallah, M.; Eltass, H.M.; Hegazy, M.A.; Ahmed, H. Adsorption and Inhibition Effect of Novel Cationic Surfactant for Pipelines Carbon Steel in Acidic Solution. *Prot. Met. Phys.Chem. Surf* **2016,** *52*, 721–730.
[17] Fouda, A.S.; Abdallah, M.; Medhat, M. Some Schiff Base Compounds as Inhibitors for Corrosion of Carbon Steel in Acidic Media. *Prot of Metals and Phys Chem of Surfaces* **2012,** *48*, 477–486.
[18] Sobhi, M.; El-Sayed, R.; Abdallah, M. The Effect of Nonionic Surfactants Containing Triazole, Thiadiazole and Oxadiazole as Inhibitors for the Corrosion of Carbon Steel in 1M Hydrochloric Acid. *J.Surf. Deterg.* **2013**, *16*, 937–946.
[19] Sobhi, M.; El-Sayed, R.; Abdallah, M. Synthesis, Surface Properties and Inhibiting Action of Novel Nonionic Surfactants on C-Steel Corrosion in 1M Hydrochloric Acid Solution. *Chem. Eng. Comm.* **2016**, *203*, 758–768.
[20] Mehdaoui, R.; Khelifa, A.; Khadraoui, A.; Aaboubi, O.; Hadj Ziane, A.; Bentiss, F.; Zarrouk, A. Corrosion Inhibition of Carbon Steel in Hydrochloric Acid Solution by Some Synthesized Surfactants from Petroleum Fractions. *Res. Chem. Interm* **2016,** *42*, 5509–5526.
[21] Hegazy, M.A.; El-Tabei, A.S.; Bedair, A.H.; Sadeq, M.A. An Investigation of Three Novel Nonionic Surfactants as Corrosion Inhibitor for Carbon Steel in 0.5M H_2SO_4. *Corros. Sci* **2012,** *54*, 219–230.
[22] Negm, N.A.; El Hashash, M.A.; Abd-Elaal, A.; Tawfik, S.M.; Gharieb, A. Amide Type Nonionic Surfactants: Synthesis and Corrosion Inhibition Evaluation Against Carbon Steel Corrosion in Acidic Medium. *J. Mol.Liq.* **2018**, *256*, 574–580.
[23] Abdallah, M.; Al-abdali, F.H.; El-Sayed, R. Protection of Aluminum Corrosion in 1.0M HCl Solution by Some Nonionic Surfactant Compounds Containing Five Membered Heterocyclic Moiety. *Chem Data Collection* **2020,** *28*, 100407.
[24] Abdallah, M.; Hegazy, M.A.; Alfakeer, M.; Ahmed, H. Adsorption and Inhibition Performance of Novel Cationic Gemini Surfactant as a Safe Corrosion Inhibitor for Carbon Steel in Hydrochloric Acid. *Green Chem. Lett. Rev* **2018,** *11*, 457–468.
[25] Alfakeer, M.; Abdallah, M.; Abdel Hameed, R.S. Propoxylated Fatty Esters as Safe Inhibitors for Corrosion of Zinc in Hydrochloric Acid. *Prot. Met. Phys. Chem. Surf* **2020,** *56*, 225–232.
[26] Fawzy, A.; Abdallah, M.; Zaafarany, I.A.; Ahmed, S.A.; Althagafi, I.I. Thermodynamic, Kinetic and Mechanistic Approach to The Corrosion Inhibition of Carbon Steel by New Synthesized Amino Acids-Based Surfactants as Green Inhibitors in Neutral and Alkaline Aqueous Media. *J . Mol. Liq* **2018,** *265*, 276–291.
[27] Fawzy, A.; Zaafarany, I.A.; Ali, H.M.; Abdallah, M. New Synthesized Amino Acids-Based Surfactants as Efficient Inhibitors for Corrosion of Mild Steel in Hydrochloric Acid Medium: Kinetics and Thermodynamic Approach. *Int. J. Electrochem Sci* **2018,** *13*, 4575–4600.
[28] Al-abdali, F.H.; Abdallah, M.; El-Sayed, R. Corrosion Inhibition of Aluminium Using Nonionic Surfactant Compounds with a Six Membered Heterocyclic Ring in 1.0M HCl Solution. *Int. J. Electrochem. Sci.* **2019**, *14*, 3509–3523.
[29] Mathur, P.B.; Vasudevan, T. Reaction-rate Studies for the Corrosion of Metals in Acids: Iron in Mineral Acids. *Corrosion.* **1982**, *38*, 17–25.
[30] Zhu, H.; Chen, X.; Li, X.; Wang, J.; Ma, X. 2-aminobenzimidazole Derivative with Surface Activity as Corrosion Inhibitor of Carbon Steel in HCl: Experimental and Theoretical Study. *J . Mol. Liq.* **2020**, *297*, 111720.
[31] Abdrabo, W.S.; Elgendy, B.; Soliman, K.A.; Abd El-Lateef, H.M.; Tantawy, A.H. Synthesis, Assessment and

Corrosion Protection Investigations of Some Novel Peptidomimetic Cationic Surfactants: Empirical and Theoretical Insights. *J. Mol. Liq.* **2020**, *315*, 113672.
[32] Abdallah, M.; Salem, M.M.; AL Jahdaly, B.A.; Awad, M.I.; Helal, E.; Fouda, A.S. Corrosion Inhibition of Stainless Steel Type 316 L in 1.0 M HCl Solution Using 1,3-Thiazolidin-5-one Derivatives. *Int. J. Electrochem Sci.* **2017**, *12*, 4543–4562.
[33] Sobhi, M.; Abdallah, M.; Khairou, K.S. Sildenafil Citrate (Viagra) as a Corrosion Inhibitor for Carbon Steel in Hydrochloric Acid Solutions. *Monatsh fur Chemie* **2012,** *143*, 1379–4562.
[34] Riggs Jr, O.L.; Hurd, R.M. Temperature Coefficient of Corrosion Inhibition. *Corrosion.* **1967**, *23*, 252–258.
[35] Laider, K.J. *Chemical Kinetics*; Mc Graw Hill, 1965.
[36] Abdallah, M.; Fawzy, A.; Hawsawi, H. Maltodextrin and Chitosan Polymers as Inhibitors for the Corrosion of Carbon Steel in in 1.0 M Hydrochloric Acid. *Int. J. Electrochem. Sci.* **2020**, *15*, 5650–5663.
[37] Abdallah, M.; Al Jahdaly, B.A. Gentamicin, Kanamycin and Amikacin Drugs as Non -Toxic Inhibitors for Corrosion of Aluminum in 1.0 M Hydrochloric Acid. *Int. J. Electrochem. Sci.* **2015**, *10*, 9808–9823.
[38] Abdallah, M.; Alfakeer, M.; Alonazi, A.M.; Al-Juaid, S.S. Ketamine Drug as an Inhibitor for the Corrosion of 316 Stainless Steel in 2M HCl Solution. *Int. J. Electrochem. Sci* **2019,** *14*, 10227–10247.
[39] Adawy, A.I.; Abbas, M.A.; Zakaria, K. New Schiff Base Cationic Surfactants as Corrosion Inhibitors for Carbon Steel in Acidic Medium: Weight Loss, Electrochemical and SEM Characterization Techniques. *Res. Chem. Intermed.* **2016,** *42*, 3385–3411.
[40] Hegazy, M.A. A Novel Schiff Base-Based Cationic Gemini Surfactants: Synthesis and Effect on Corrosion Inhibition of Carbon Steel in Hydrochloric Acid Solution. *Corros. Sci.* **2009**, *51*, 2610–2618.
[41] Bedir, A.G.; El-raouf, M.A.; Abdel-Mawgoud, S.; Negm, N.A.; El Basiony, N.M. Corrosion Inhibition of Carbon Steel in Hydrochloric Acid Solution Using Ethoxylated Nonionic Surfactants Based on Schiff Base: Electrochemical and Computational Investigationsm. *ACS Omega* **2021,** *6*, 4300–4312.
[42] Fouda, A.S.; Zaki, E.G.; Khalifa, M.M.A. Some new Nonionic Surfactants Based on Propane Tricarboxylic Acid as Corrosion Inhibitors for Low Carbon Steel in Hydrochloric Acid Solutions. *J. Bio- and Tribo-Corros.* **2019**, *5*. Article number: 31.
[43] Abdallah, M.; Helal, E.A.; Fouda, A.S. Amino Pyrimidine Derivatives as Inhibitors for Corrosion of 1018 Carbon Steel in Nitric Acid Solutions. *Corros. Sci.* **2006**, *48*, 1639–1654.
[44] Schmitt, G., Proceedings of the Sixth European Symposium on Corrosion inhibitors (6 SEIC), Ann Univ, Ferrara, N.S. Sez Suppl N. 8, 1985, Separate paper.
[45] Chattaraj, P.K. *Chemical Reactivity Theory: A Density Functional View*; CRC Press. Taylor & Francis: libgen.lc, 2009.
[46] Parr, R.G.; Yang, W. *Density Functional Theory of Atoms and Molecules*; Oxford University Press: New York, 1989.
[47] De Proft, F.; Geerlings, P. Conceptual and Computational DFT in the Study of Aromaticity. *Chem. Rev* **2001,** *101*, 1451–1464.
[48] Geerlings, P.; De Proft, F.; Langenaeker, W. Conceptual Density Functional Theory. *Chem. Rev.* **2003**, *103*, 1793–1874.
[49] Geerlings, P.; Fias, S.; Boisdenghien, Z.; De Proft, F. Conceptual DFT: Chemistry from the Linear Response Function. *Chem. Soc. Rev* **2014,** *43*, 4989–5008.
[50] Frau, J.; Glossman-Mitnik, D. Conceptual DFT Descriptors of Amino Acids with Potential Corrosion Inhibition Properties Calculated with the Latest Minnesota Density Functionals. *Front Chem.* **2017**, *5*. Article 16.
[51] Bentiss, F.; Lebrini, M.; Vezin, H.; Lagrenee, M. Experimental and Theoretical Study of 3-Pyridyl-Substituted 1,2,4-Thiadiazole and 1,3,4-Thiadiazole as Corrosion Inhibitors of Mild Steel in Acidic Media. *Matt. Chem. Phys.* **2004,** *87*, 18–23.
[52] Wang, H.; Wang, X.; Wang, H.; Wang, L.; Liu, A. DFT Study of New Bipyrazole Derivatives and Their Potential Activity as Corrosion Inhibitors. *J. Mol. Model* **2007,** *13*, 147–153.
[53] Allam, N.K. Thermodynamic and Quantum Chemistry Characterization of the Adsorption of Triazole Derivatives During Muntz Corrosion in Acidic and Neutral Solutions. *App. Surf. Sci* **2007,** *253*, 4570–4577.
[54] Sahin, M.; Gece, G.; Kaerci, F.; Bligic, S. Experimental and Theoretical Study of the Effect of Some Heterocyclic Compounds on the Corrosion of low Carbon Steel in 3.5% NaCl Medium. *J. Appl. Electrochem* **2008,** *38*, 809–815.
[55] Cruz, J.; García-Ochoa, E.; Castro, M. Corrosion, Passivation, and Anodic Films-Experimental and Theoretical Study of the 3-Amino-1, 2, 4-Triazole and 2-Aminothiazole Corrosion Inhibitors in Carbon Steel. *J. Electrochem. Soc.* **2003,** *150*, B26.
[56] Gázquez, J.L.; Cedillo, A.; Vela, A. Electrodonating and Electroaccepting Powers. *J. Phys. Chem. A.* **2007,** *111*, 1966–1970.
[57] Domingo, L.R.; Pérez, P. The Nucleophilicity *N* Index in Organic Chemistry. *Org. Biomol. Chem* **2011,** *9*, 7168–7175.
[58] Chauhan, L.R.; Gunasekaran, G. Corrosion Inhibition of Mild Steel by Plant Extract in Dilute HCl Medium. *Corros. Sci* **2007,** *49*, 1143–1167.
[59] Wahyuningrum, D.; Achmad, S.S.; Buchari, Y.M.; Bundjali, B.; Ariwahjoedi, B. The Correlation Between Structure and Corrosion Inhibition Activity of 4,5-Diphenyl-1-Vinylimidazole Derivative Compounds Towards Mild Steel in 1% NaCl Solution. *Int. J. Electrochem. Sci* **2008,** *3*, 154–166.
[60] Benmessaoud, M.; Es-Salah, K.; Hajjaji, N.; Takenouti, H.; Srhiri, A.; Ebentouhami, M. Inhibiting Effect of 2-Mercaptobenzimidazole on the Corrosion of Cu–30Ni Alloy in Aerated 3% NaCl in Presence of Ammonia. *Corros. Sci* **2007,** *49*, 3880–3888.
[61] Rodríguez-Valdez, L.M.; Villamisar, W.; Casales, M.; González-Rodríguez, J.G.; Martínez-Villafañe, A.; Martínez, L.; Glossman-Mitnik, D. Computational Simulations of the Molecular Structure and Corrosion Properties of Amidoethyl, Aminoethyl and Hydroxyethyl Imidazolines Inhibitors. *Corros. Sci* **2006,** *48*, 4053–4064.
[62] Gómez, B.; Likhanova, N.V.; Domínguez-Aguilar, M.A.; Martínez-Palou, R.; Vela, A.; Gázquez, J.L. Quantum Chemical Study of the Inhibitive Properties of 2-Pyridyl-Azoles. *J. Phys. Chem. B.* **2006**, *110*, 8928–8934.